

Applications and experiments

Balassa Gábor

Msc seminar

Contents

- What have we learnt so far?
- Applications of the mesoscopic theory.
- Experiment setups, instrumentation...

Summary

- Scattering theory
- DC and AC currents in mesoscopic transport theory
- **Noises**
 - **Thermal noise**
 - **Shot noise**
 - **1/f noise**

Applications of the mesoscopic theory

- Quantum point contacts
- Metallic diffusive wires: transport in multi channel diffusive wires in the metallic regime.
 - Wire length is longer than the mean free path
 - All electron states localized in the presence of a disorder
localization length = number of transverse channels * mean free path
- Quantum Hall conductor
- Quantum dots: 1D channel constrained by two barriers -> when the barriers are close to each other -> 0D system between the barriers.

Quantum point contact

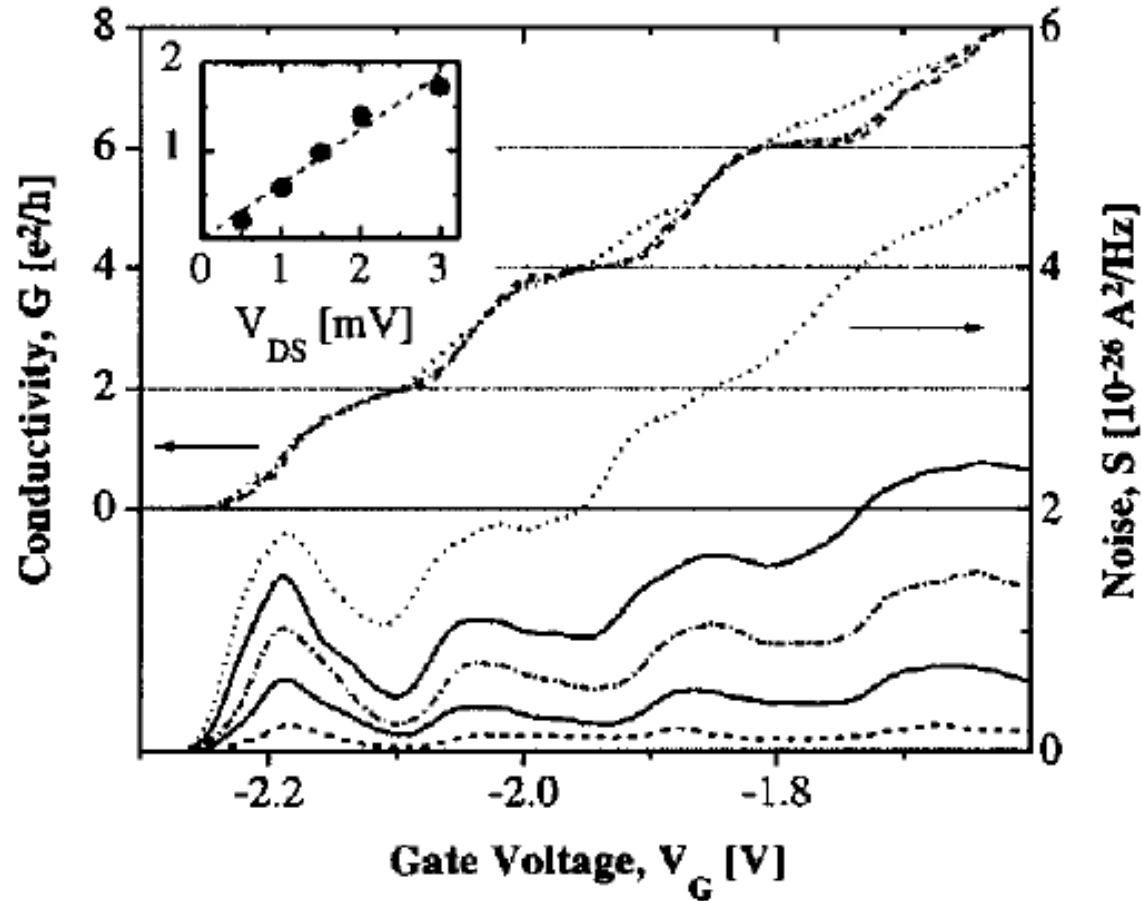


FIG. 7. Conductance (upper plot) and shot noise (lower plot) as functions of the gate voltage, as measured by Reznikov *et al* [42]. Different curves correspond to five different bias voltages.

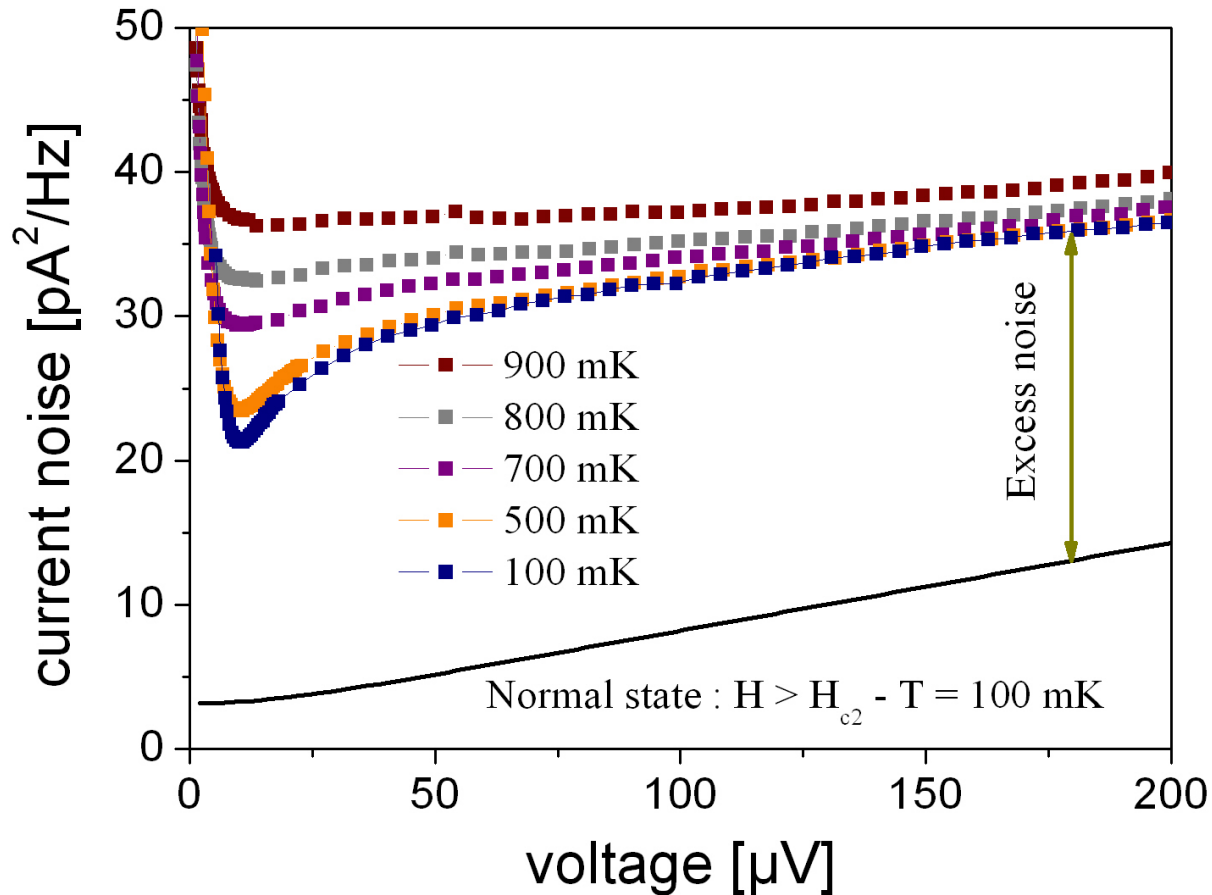
Shot noise:

- V_g dependent
- Exponentially suppressed near the plateaus
- Identical spikes between the plateaus.
- Disappears when inelastic scattering becomes significant.

Shot noise in mesoscopic conductors

- Landauer-Buttiker formalism \rightarrow conductance is the trace of the transmission matrix.
- Conservation of quantum coherence of the wave functions.
- Inelastic collisions \rightarrow fluctuations (transmitted current) \rightarrow shot noise
- Shot noise is very sensitive to interactions
- Proportionality to the charge of the current carriers.

Thouless energy : characteristic energy scale of diffusive disordered conductors. Sensitivity to boundary conditions.



Samples: diffusive conductors

Contact with on or two superconductors.

Proximity effect \rightarrow conductor acquires supercond. Properties \rightarrow charge of the carriers is greater \rightarrow greater shot noise!

Resonant tunnel barriers

- Nonlinear transport through one 1D barrier
- Assumption: resonant states inside the barrier (randomly distr.)
- Impurities in the barrier->Transition rates are extremely sensitive
- Double barrier model -> impurity is a potential well.
- Tunneling rate depends on the impurities(->resonances)

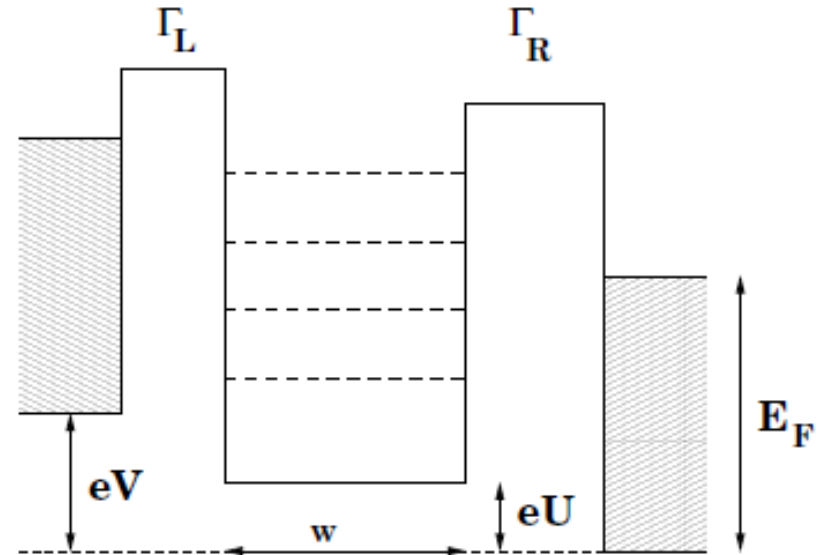


FIG. 8. Resonant double barriers. The case of low voltage is illustrated; resonant levels inside the well are indicated by dashed lines.

- Fano factor: measure of the dispersion of a distribution function.
- It results from the energy loss in a collision (in the detector) not being purely statistical.

$$F = \frac{\sigma_W^2}{\mu_W},$$

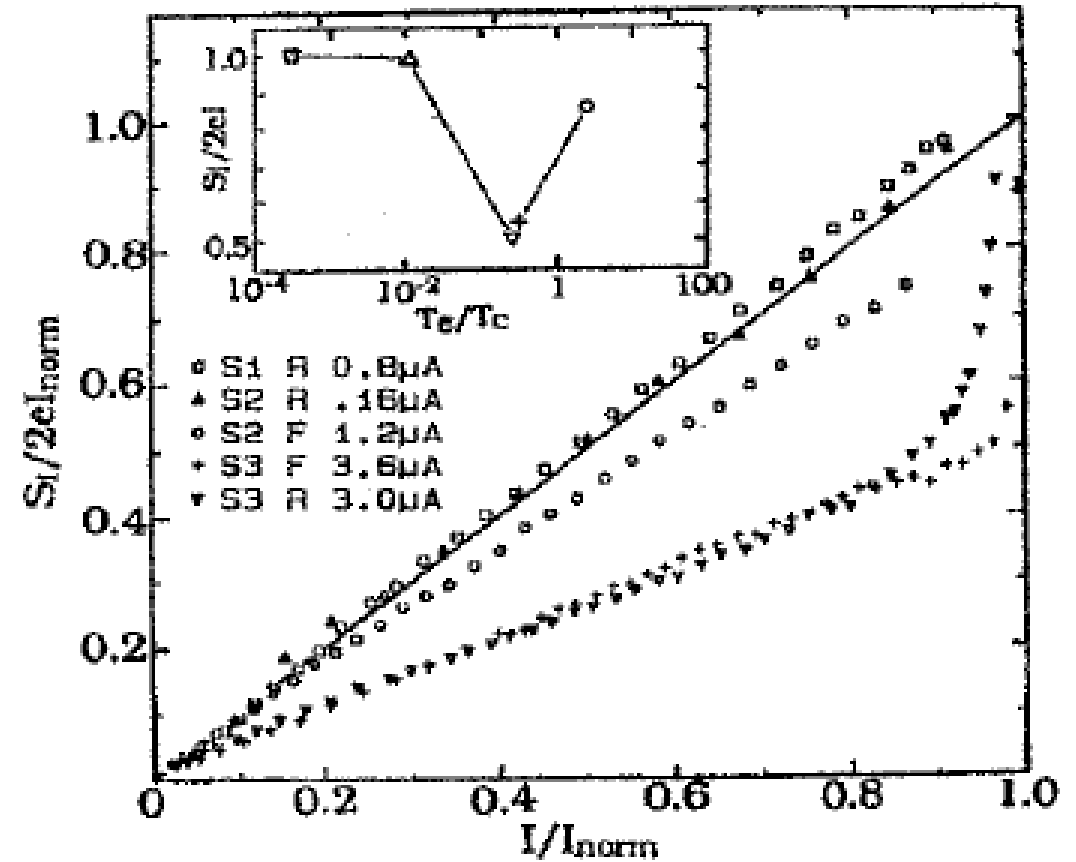


FIG. 9. The Fano factor observed experimentally by Li *et al* [64] as a function of current for three quantum wells, which differ by their asymmetry. The solid line represents the Poisson shot noise value.

Metallic diffusive wires

T=0 shot noise power:
$$S = \frac{e^3 |V|}{3\pi\hbar} \frac{N_{\perp} l}{L} = \frac{1}{3} S_P.$$

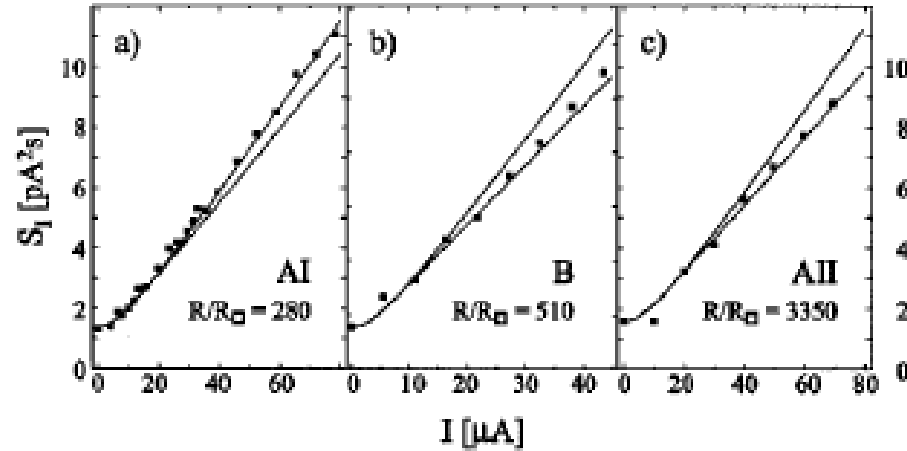


FIG. 11. Shot noise measurements by Henny *et al* [81] on three different samples. The lower solid line is 1/3-suppression, the upper line is the hot-electron result $F = \sqrt{3}/4$ (see Section VI). The samples (b) and (c) are short, and clearly display 1/3-suppression. The sample (a) is longer (has lower resistance), and the shot noise deviates from the non-interacting suppression value due to inelastic processes.

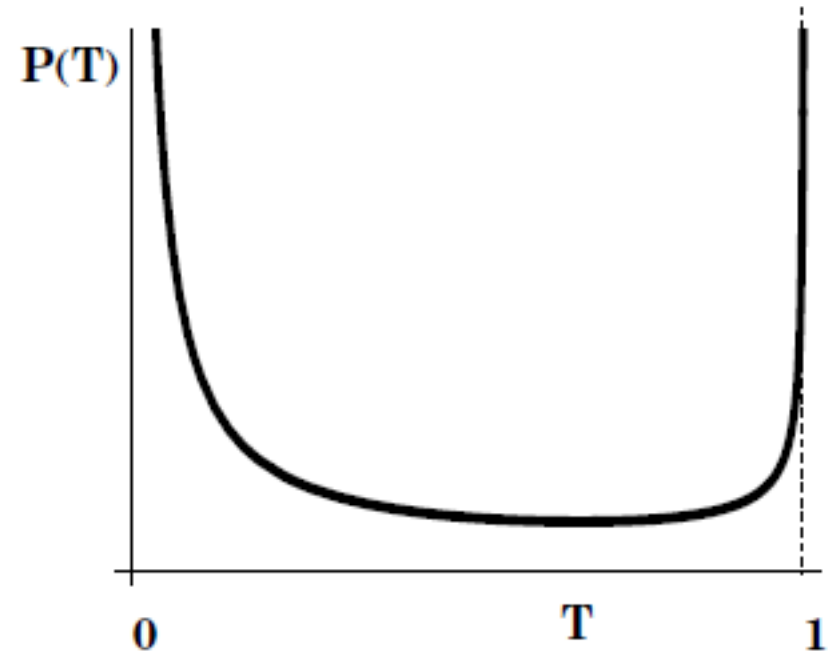
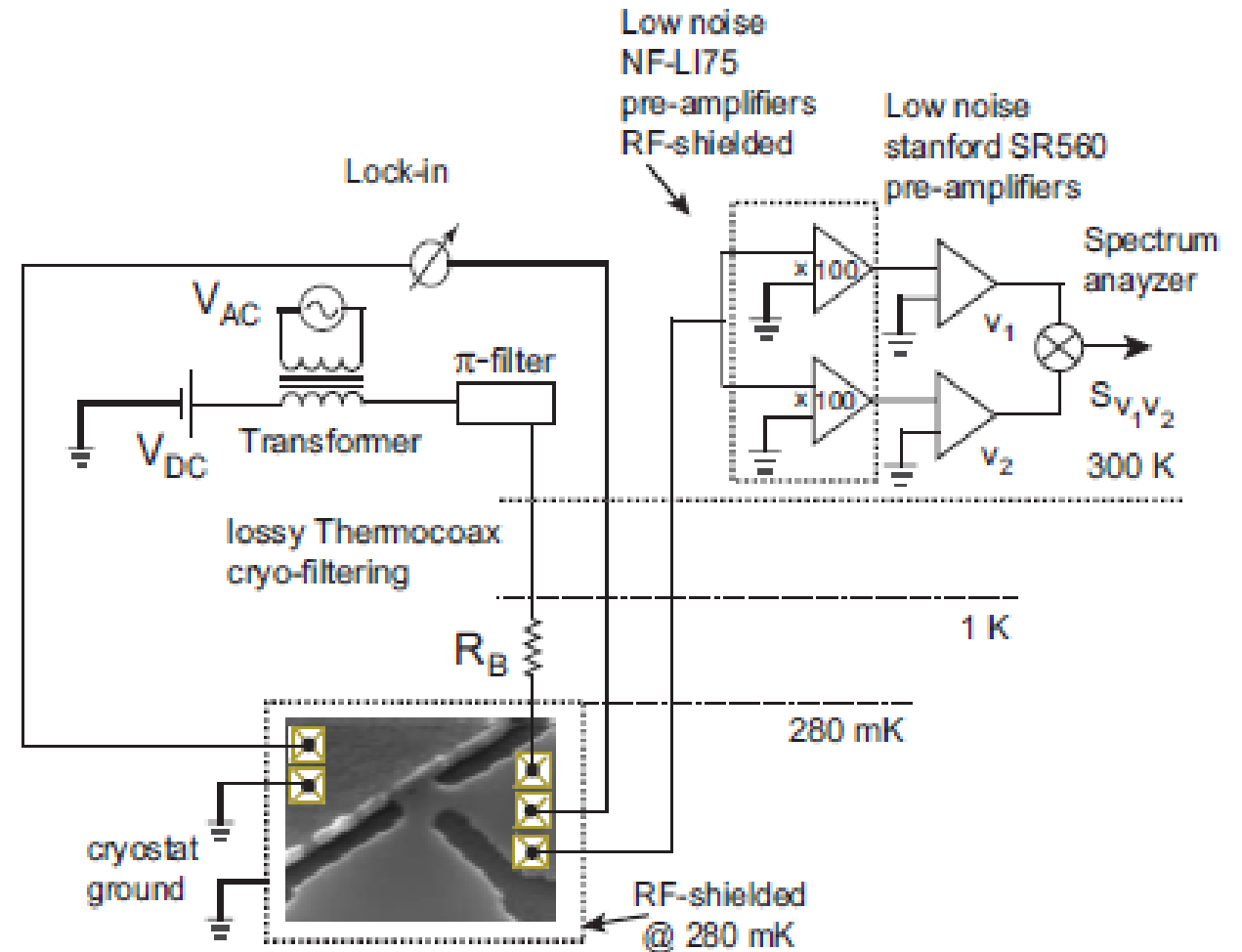


FIG. 10. Distribution function of transmission coefficients (87) for $L/l = 10$.

Experimental setup

- Low temperature : N2 (77K) to pre cool the cryostat or to keep the cooling of the outer jacket.
- Noise measurement: Generators, Low noise amplifiers, spectrum analyser, filters, shielding, Lock in ...



$$\begin{aligned}
 \langle V_1 V_2 \rangle &= \langle V_S^2 \rangle + R_S(R_S + R_L)i_1^2 + R_S(R_S + R_L)i_2^2 \\
 &= \langle V_S^2 \rangle + 2R_S^2 \cdot i_{Amp}^2.
 \end{aligned}$$

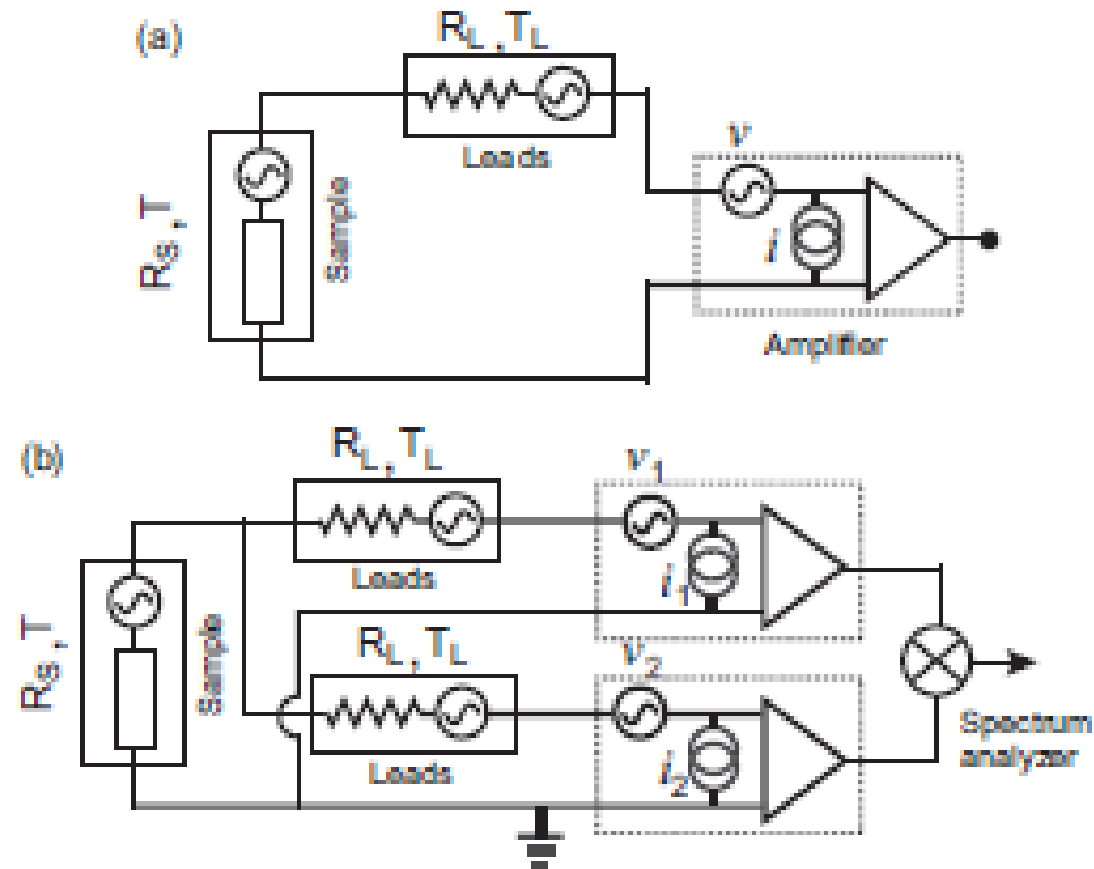
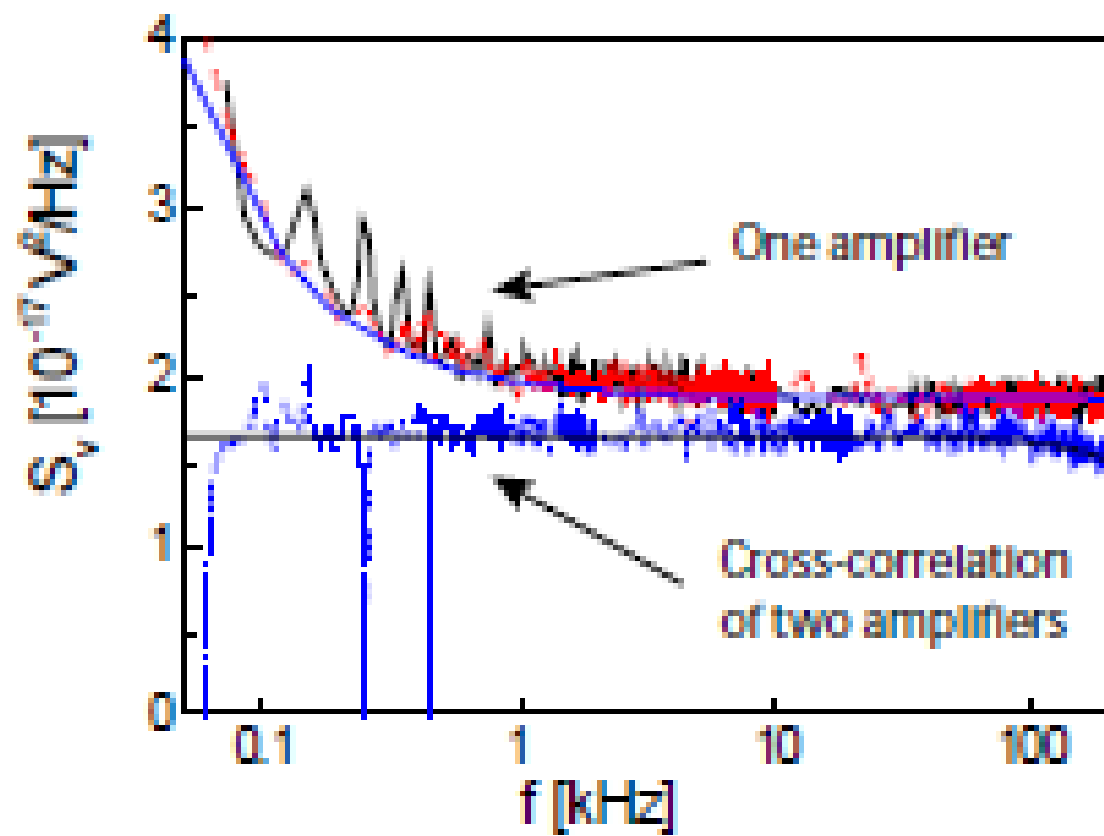
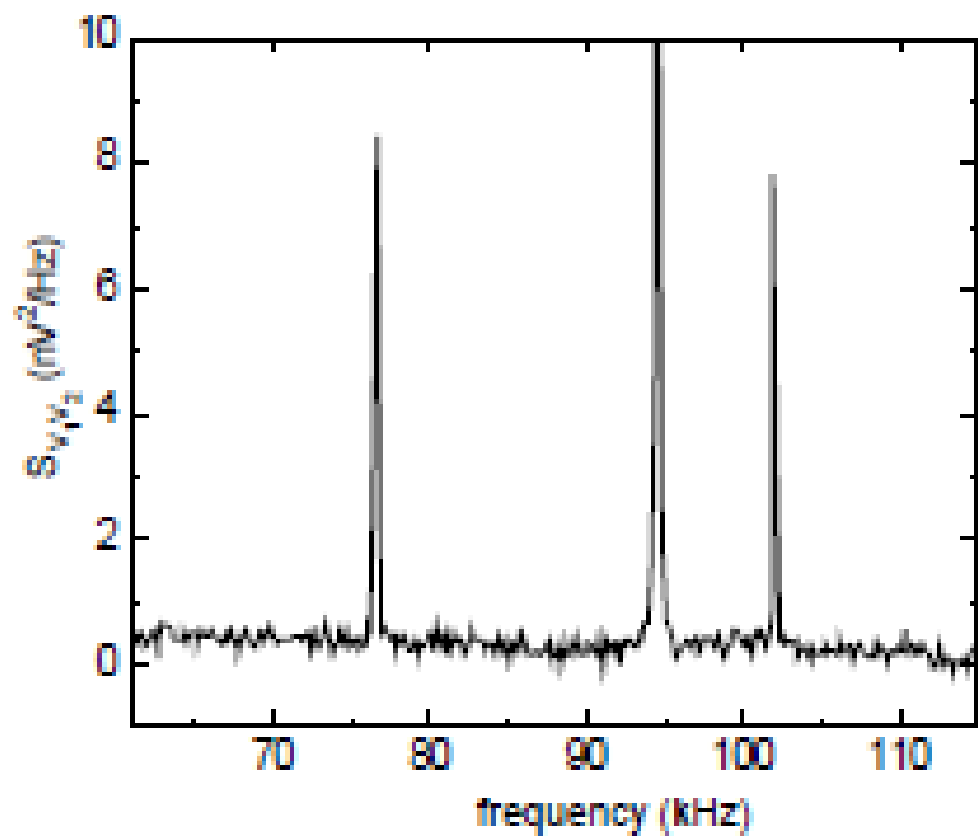


Figure 4.3: (a) Conventional way of noise detection circuit with one amplifier. (b) Cross-correlation technique, analogous to the four-point method in resistance measurements with two amplifiers in parallel.



Electron heating effects in diffusive metallic wires

- Current flow in a mesoscopic wire
-> T_e rises above the phonon temperature -> at low temperatures it can influence the measurements.
- Electric noise measurement -> electron heating
- Au wires on oxidized Si wafers
- Voltage is amplified with two low noise amplifiers.

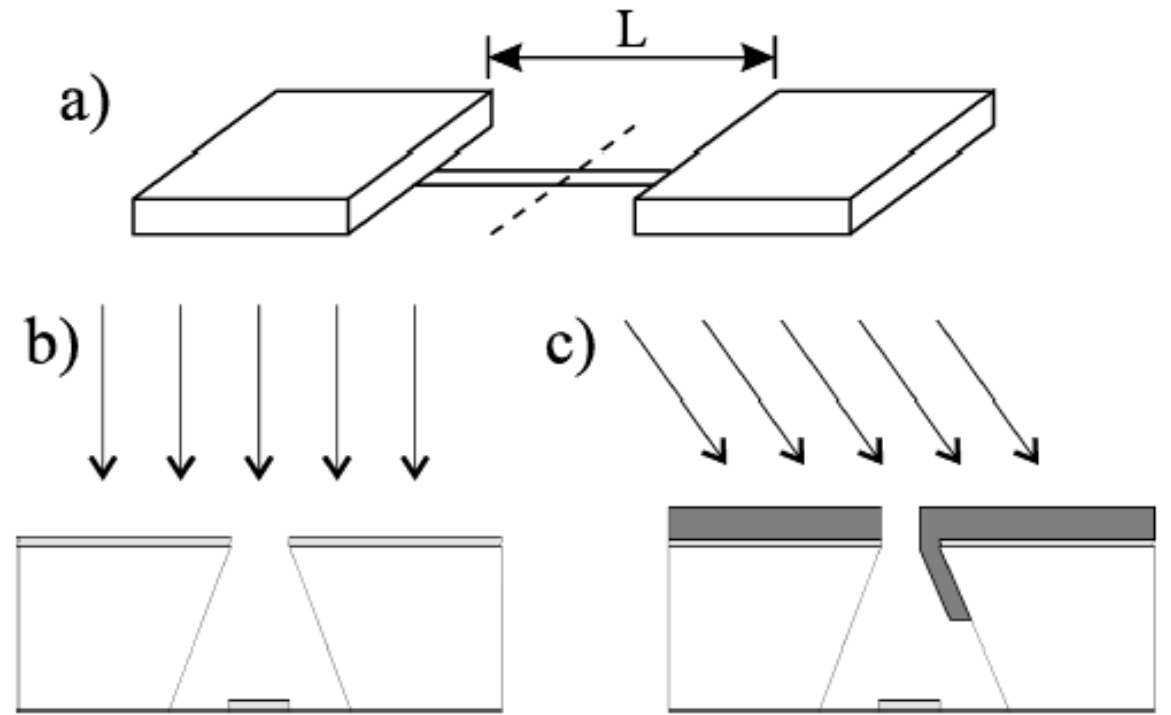


FIG. 1. (a) Schematic of the wire fabricated for noise measurements; (b) perpendicular evaporation of the wire material, (c) evaporation of thick reservoirs under a tilt angle; and (b) and (c) are cross sections along the dashed line in (a).

- Cross correlation noise measurement with spectrum analyser.

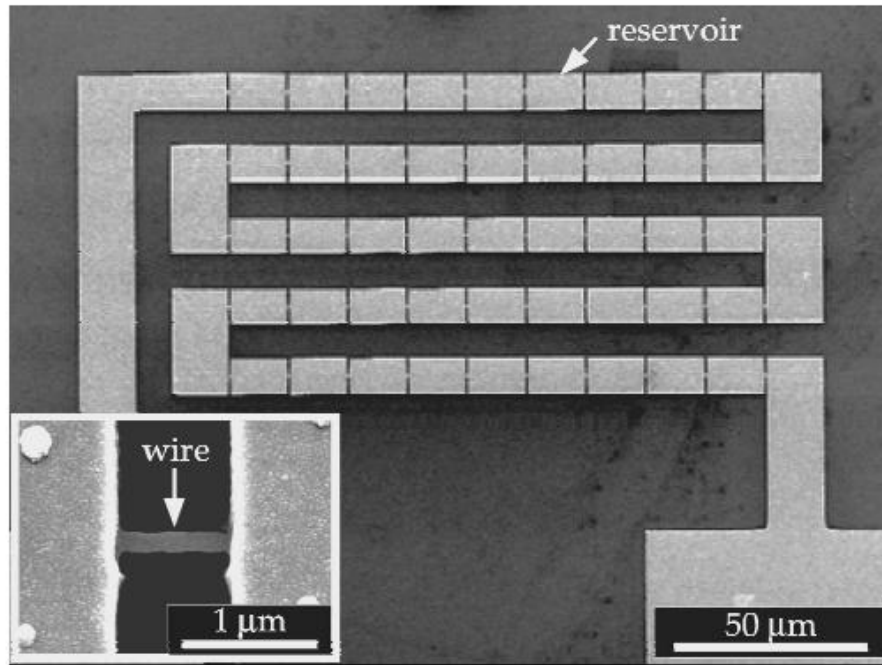


FIG. 2. 50 wires with a length of 840 nm and a width of 140 nm each with large, thick thermal reservoirs in between, were fabricated using the technique illustrated in Fig. 1. The inset shows one single wire.

Cooling of the reservoirs are very effective

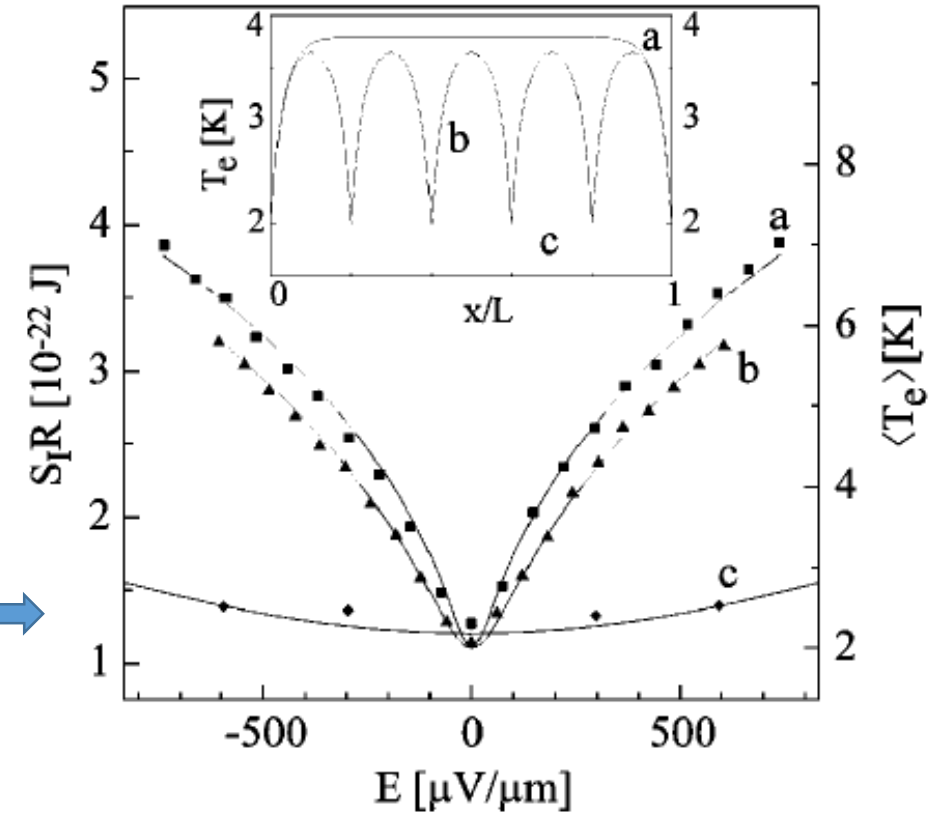


FIG. 3. Measured noise power and corresponding electron temperature versus applied electric field for three different samples. Sample A is a 50 μm long Au wire ($R=812 \Omega$, width $w=110 \text{ nm}$), sample B consists of five wires of 10 μm length in series ($R=667 \Omega$, $w=120 \text{ nm}$), sample C consists of 30 wires with a length of 0.84 μm ($R=300 \Omega$, $w=140 \text{ nm}$). a–c corre-

- Electron temperature depends crucially on the length of the wires and the presence of thermal reservoirs.
- Noise measurement is an effective tool to measure electron heating effects.

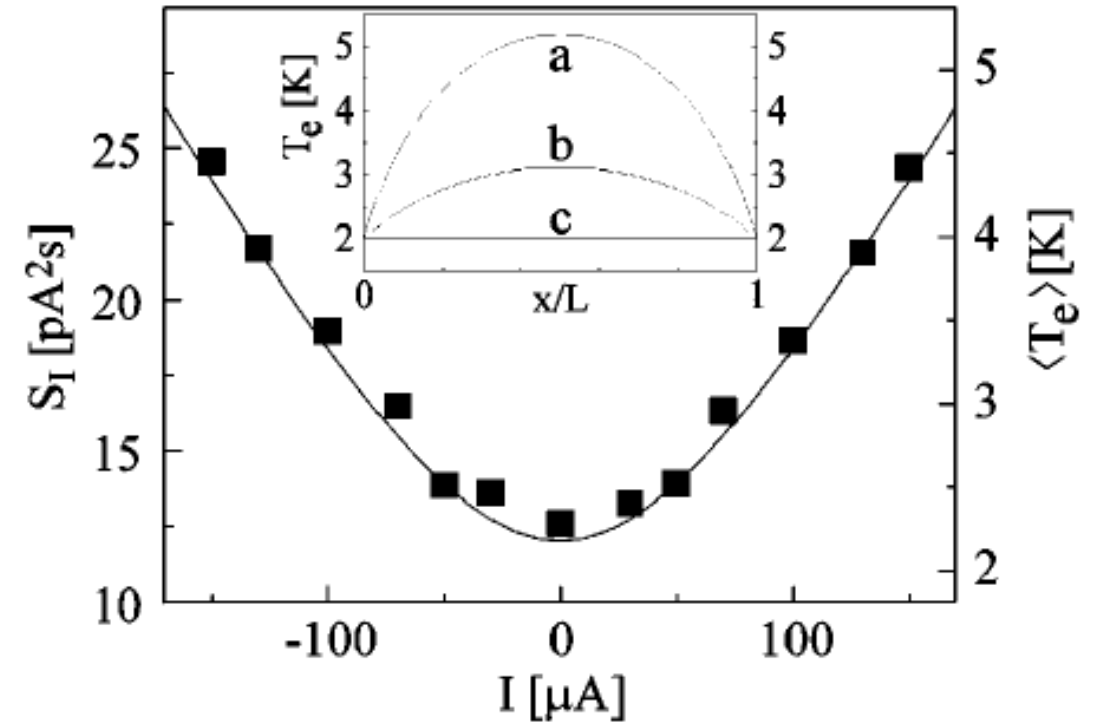


FIG. 4. Noise measurement of sample C of Fig. 3 (30 wires in series with a length of 840 nm). The solid line is the prediction of Eq. (2), which has no adjustable fit parameter. The inset shows the temperature profile of a single wire for 0, 75, and 150 μA (from bottom to top).

Thank you for your attention